300
7-12-65

UNCLASSIFIED

GEMP-48A

MASTER

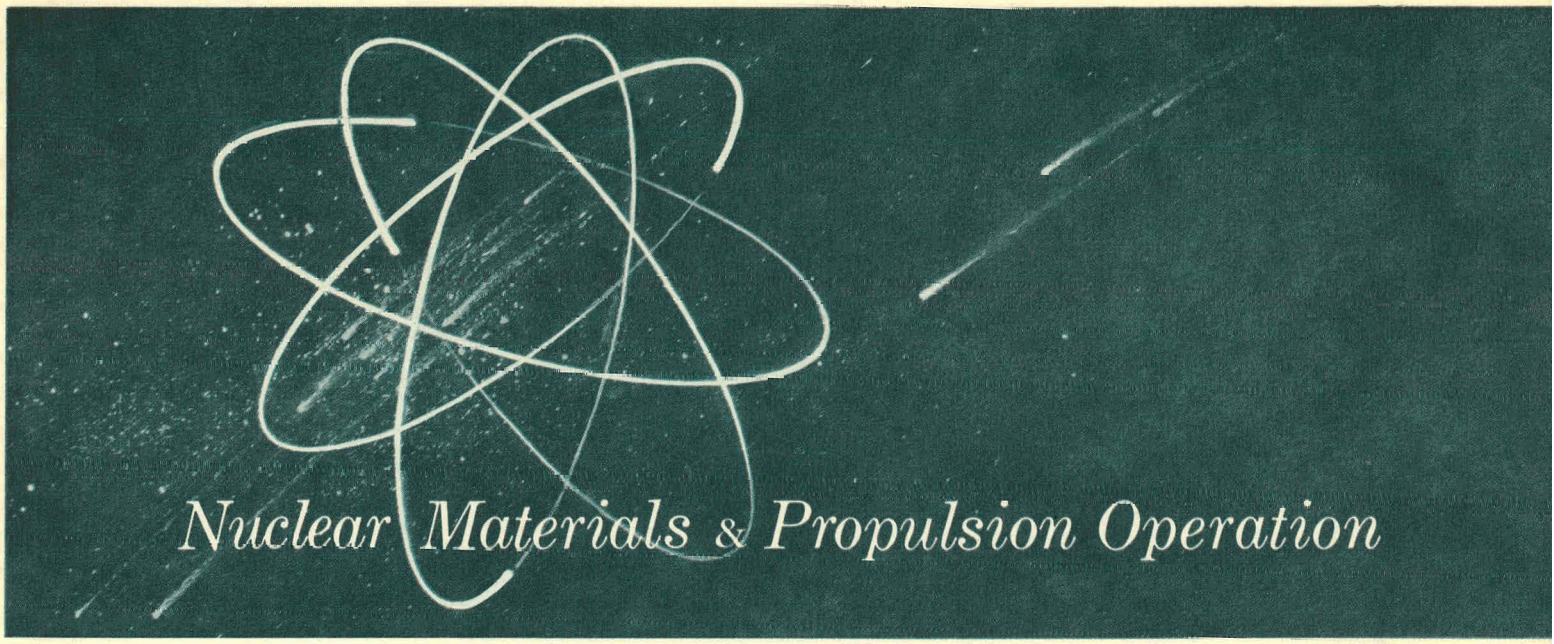

HIGH-TEMPERATURE MATERIALS PROGRAM
PROGRESS REPORT No.48, Part A

June 25,1965

GENERAL ELECTRIC

ATOMIC PRODUCTS DIVISION

UNCLASSIFIED

DISCLAIMER

Printed in USA. Price $2.00. Available from the

Clearinghouse for Federal Scientific and
Technical Information,
National Bureau of Standards,
U. S. Department of Commerce,
5285 Port Royal Road,
Springfield, Virginia 22151

GEMP-48A

UC-25 Metals, Ceramics, and Materials
TID-4500 (42nd Ed.)

HIGH-TEMPERATURE MATERIALS PROGRAM
PROGRESS REPORT No.48, Part A

June 25,1965

United States Atomic Energy Commission Contract No. AT(40-1)-2847

NUCLEAR MATERIALS and PROPULSION OPERATION
ATOMIC PRODUCTS DIVISION

GENERAL ELECTRIC

Cincinnati 15, Ohio

DISTRIBUTION

EXTERNAL

AEC Headquarters
G. K. Dicker W. R. Voigt
F. C. Schwenk G. W. Wensch
J. M. Simmons M. J. Whitman

AEC, CANEL Project Office
A. J. Alexander

AEC, CAO
C. L. Karl J. F. Weissenberg

AEC, OROO
D. F. Cope (3) D. S. Zachry, Jr.

AEC, SAN
Col. J. B. Radcliffe, Jr.

Argonne National Laboratory
R. Noland

Atomics International
S. C. Carniglia C. E. Weber

Battelle - Northwest
F. W. Albaugh R. E. Nightingale
J. J. Cadwell

BMI
S. Paprocki

Chase Brass and Copper
J. Port

General Atomic
D. Ragone

Institute for Defense Analyses
R. C. Hamilton

Jet Propulsion Laboratory
J. Davis

LASL
R. D. Baker

Lawrence Radiation Laboratory
C. Cline A. J. Rothman

NASA Headquarters
J. J. Lynch

NASA, Lewis Research Center
J. W. Creagh T. A. Moss N. Saunders
T. P. Moffitt L. Rosenblum N. D. Sanders
H. Schwartz

ORNL
R. E. Blanco W. O. Harms
W. R. Grimes P. Patriarca (2)

Pratt and Whitney Aircraft (CANEL)
L. M. Raring (3)

Universal-Cyclops Steel Corp.
L. M. Bianchi

Wah Chang Corporation
S. Worchester

Westinghouse, Astronuclear Lab.
D. C. Goldberg

INTERNAL

E. A. Aitken
W. G. Baxter
J. R. Beeler
J. C. Blake
K. M. Bohlander
B. Bonini
H. C. Brassfield
R. W. Brisken
V. P. Calkins
C. L. Chase (3)
K. P. Cohen, APD
C. G. Collins (2)
E. S. Collins
J. F. Collins
P. K. Conn
J. B. Conway
E. B. Delson
H. S. Edwards
E. W. Filer
R. E. Fryxell
E. S. Funston
G. F. Hamby
J. O. Hibbits
A. N. Holden, APED (2)
R. E. Honnell
L. D. Jordan
G. Korton
W. H. Long
L. R. McCreight, MSD
J. W. Morfitt
J. Moteff
R. E. Motsinger
G. T. Muehlenkamp
C. E. Niemeyer
W. E. Niemuth
G. W. Pomeroy
W. Z. Prickett
F. C. Robertshaw
E. J. Schmidt, ATS
L. H. Sjodahl
R. J. Spera
C. L. Storrs
P. P. Turner
F. O. Urban
H. Wagner
J. F. White
V. C. Wilson, RL
O. G. Woike
R. E. Wood
J. F. Young, APD
Library (10)

CONTENTS

FIGURES

TABLES

CONVERSION TABLE

To Convert From	To	Multiply By
Atmospheres	Pounds/inch^2	14.7
Calories (mean)	Btu (mean)	0.00397
Calories/gram-^oC	Btu/pound-^oF	1.0
Calories/sec-cm-^oC	Btu/hr-ft-^oF	241.8
Calories/sec-cm^2	Btu/hr-ft^2	1.32 x 10^4
Calories/sec-cm^2-^oC	Btu/hr-ft^2-^oF	7370
Centimeters	Feet	0.03281
	Inches	0.3937
Cubic centimeters	Cubic feet	3.531 x 10^{-5}
	Cubic inches	0.06103
Grams	Pounds	0.002205
Grams/cm^3	Pounds/ft^3	62.43
Grams/cm^2	psi	0.01422
Kilograms	Pounds	2.205
Kilograms/cm^2	Atmospheres	0.9678
	Pounds/ft^2	2048
	Pounds/inch^2	14.22
Kilograms/mm^2	Pounds/inch^2	1422.32
Kilowatts	Btu/sec	0.948
Liters	Cubic feet	0.0353
Meters	Inches	39.37
Millimeters of mercury	Atmospheres	0.001316
Square centimeters	Square feet	0.001076
	Square inches	0.155
Torr	mm of Hg	1.0
	Atmospheres	0.001316
Watts/cm-^oC	Btu/hr-ft-^oF	57.8
Watt-seconds	Btu	0.000948
Watts/cm^2	Btu/hr-ft^2	3170
Watts/cm^2-^oC	Btu/hr-ft^2-^oF	1760
Centimeters/sec	Feet/sec	0.03281
Meters/sec	Feet/sec	3.281

1. INTRODUCTION AND SUMMARY

Introduction

This report is the unclassified portion of the forty-eighth in a series of monthly reports of the work in process on materials research and development for the Atomic Energy Commission under Contract AT(40-1)-2847.

Included is a summary of the work from March 15, 1965 to May 15, 1965, on four of the specific research and development efforts in process. Four of the remaining programs are reported in the classified portion of this report, GEMP-48B.

Six other research and development efforts covered by the contract are reported in alternate months.

Summary

FISSION PRODUCT TRANSPORT PROCESSES IN REFRACTORY-METAL FUEL SYSTEMS (57070)

Krypton was concurrently dissolved and diffused in tantalum cathode samples which were self-resistively heated to 1730°C while under glow discharge for different exposure times and pressures. These diffusion samples were sectioned in 400 Å-thick sections. The data obtained suggested that a constant surface concentration is maintained during the experiments (up to 10 minutes) and that the data could be analyzed using an error function solution to the diffusion equation. Analysis of the data indicated that, under the test conditions used, diffusion along high diffusivity paths was the dominant transport process beyond about 400 Å.

INTERNAL CONVERSION FUEL ELEMENT RESEARCH (57072)

Two ETR irradiation tests of fuel elements containing 25 volume percent UO_2-ThO_2-Y_2O_3 are continuing on test after satisfactorily operating for 2500 hours at 1250°C. Post-irradiation analysis of the in-pile ducting used with LITR test LTC-73 of fueled BeO at temperatures up to 1550°C confirmed previous indications that the dominant fission product release process is recoil.

Chemical analysis of UO_2-ThO_2 and UO_2-ThO_2-Y_2O_3 fueled-BeO specimens that completed extended fuel retention tests at high temperatures in various atmospheres confirmed the excellent stability of the Y_2O_3-containing compositions.

RADIATION EFFECTS IN BeO (57063)

Measurement procedures for determining bulk volume and density and open and total porosity of ceramic specimens to a precision of ±0.1 percent are described. The procedure is similar to that described in ASTM method C 20-46 but utilizes vacuum impregnation with toluene and diethylphthalate fluids rather than water.

Density and porosity measurements of unirradiated specimens representative of the compositions, grain sizes, and densities used in the irradiation studies showed that, in general, the open porosity exceeded 1 percent only if the total porosity was greater than 10 to 12 percent.

Post-irradiation measurements on additional specimens containing glass-phase additives provided further evidence that these additives lead to slightly increased expansion at irradiation temperatures of 900^{o} to 1000^{o}C.

Electron micrographs of polished sections of the 20-micron grain size AOX and EBOR samples irradiated at 1000^{o}C to 2.5 to 3 x 10^{21} nvt ($\geq$ 1 Mev) failed to yield evidence of microcracking. Additional examinations are in progress; however, it appears now that these are the first irradiated specimens to exhibit a decrease of 20 to 40 percent in strength in the absence of microcracking.

2. FISSION GAS DIFFUSION IN UNFUELED CERAMIC MATERIALS (57069)

The objective of this program is to advance the basic knowledge of fission gas diffusion and radiation damage in unfueled ceramic materials.

This work is concerned with the diffusion of Kr, Xe, and I atoms in ceramic oxides (MgO, BeO, Al_2O_3, and ZrO_2) subsequent to their injection via ion bombardment. The diffusion characteristics of these heavy atoms are deduced by an analysis of the amount of diffusant remaining in a sample as a function of time at constant temperature.

ION BOMBARDMENT STUDIES

The use of a washer-type target holder with its surface discontinuities was shown previously[1] to destroy beam uniformity at the target. However, retention of beam uniformity has been achieved by employing a target holder with individually recessed holes for target placement. The depth and diameter of these holes are just sufficient to receive the ceramic targets and form essentially a planar surface for ion impact. Maximum variation in krypton inventory was no greater than 8 percent among BeO targets injected in this manner.

The krypton release from these targets is currently being measured at 1000°C with release measurements at higher temperatures to follow. The release data obtained, however, will be from a highly damaged material since 3.7×10^{14} ion impacts/cm^2 were required to attain a level of radioactivity adequate for counting statistics. To obtain material with less damage, the Kr^{85} enrichment of the bombarding gas has been increased so that ion impacts of 10^{11} ions/cm^2 will be sufficient for radioactive assay of targets with impact areas of 0.28 cm^2.

In the past, the total ion beam current was obtained by integrating time versus current curves of a recording micromicroammeter. This method has been replaced by a current integrator of the following type: the ion beam charges an 0.1 microfarad capacitor connected between the Faraday cage and ground, and the number of ions striking the cup are calculated from the measured voltage drop across the capacitor and its capacitance. Charge build-up on the capacitor by secondary electron emission from the cup during bombardment is suppressed by biasing the cup + 10 volts prior to the start of an irradiation.

WORK PLANNED FOR NEXT PERIOD

Krypton inventory changes in BeO target specimens will be investigated as a function of time at constant temperature and initial inventory.

[1] "High-Temperature Materials Program Progress Report No. 46, Part A," GE-NMPO, GEMP-46A, April 15, 1965, pp. 9–10.

3. FISSION PRODUCT TRANSPORT PROCESSES IN REFRACTORY-METAL FUEL SYSTEMS

(57070)

The purpose of this program is to study fission product transport processes in refractory-metal fuel systems at temperatures exceeding 1700°C in inert or reducing atmospheres.

As part of the overall evaluation of refractory metals for reactor applications, both fission product migration and the effect of fission product impurities on the mechanical properties of refractory metals and their alloys are being investigated. The current work is divided into four major areas: (1) diffusion of rare gases (Kr^{85}) in arc-cast tantalum, (2) permeation of rare gases (Kr^{85}) through arc-cast tantalum, (3) transport of fission products in refractory metals, and (4) effect of fission product impurity atoms on mechanical properties of refractory metals.

RARE GAS DIFFUSION STUDIES

The diffusion of rare gases in refractory metals is being studied by concurrent solution and diffusion of krypton (containing Kr^{85}) in resistively heated arc-cast tantalum cathodes subjected to glow discharge. The cathode specimens are stripped in thin sections and the change in beta activity determined. Modification to the vacuum system, resulting in a cleaner atmosphere during glow discharge, permits initial sections as thin as 100 Å to be removed. The thickness of the section was estimated from the applied voltage for anodization of the sample and the limiting voltage thickness.[1] The beta count rates on both sides of the sample after each sectioning were in satisfactory agreement.

Absorption and diffusion of krypton in fine-grained (~16 microns) tantalum sheet samples were attained under glow discharge at an applied voltage of 300 volts and a constant temperature of 1730°C. Based on the autoradiographic results from one sample, the areal distribution of krypton is assumed to be uniform. Variations of both time (5 and 10 minutes) and pressure (0.05 to 0.24 Torr) did not have an appreciable effect on the surface concentration or on the distribution profile of the krypton. This suggests that (1) a constant surface concentration is maintained during the experiments, at least until pronounced grain growth apparently causes depletion of the concentration, and (2) that the data can be analyzed using an error function[2] solution to the diffusion equation. Typical data for fine-grained (~16 microns) material are shown in Figures 3.1 and 3.2 in which the logarithm of beta activity is plotted versus distance into the sample and the square-of-distance into sample, respectively; the data points are plotted at the midpoint of the section removed.

As indicated by the data in the figures, the distribution of krypton from beyond the first 400 Å-thick-section is linear with distance into the sample rather than with square-

[1] "Fourth Annual Report – High-Temperature Materials and Reactor Component Development Programs, Volume I – Materials," GE-NMPO, GEMP-334A, February 26, 1965, p. 176.

[2] A. J. Mortlock, "Anomalous Volume Diffusion in the Surface Layers of Metals," *Acta Metallurgica*, Volume 12, 1964, p. 675.

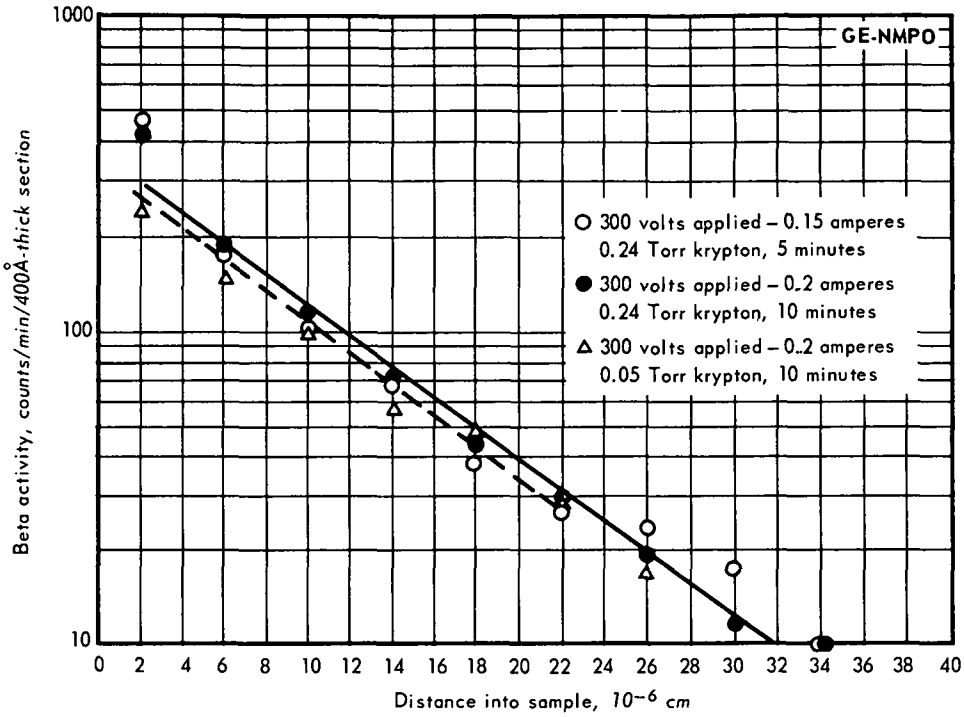

Fig. 3.1 – Distribution of Kr^{85} in arc-cast tantalum sheet samples (~16μ grain size) following absorption and diffusion under glow discharge at 1730°C

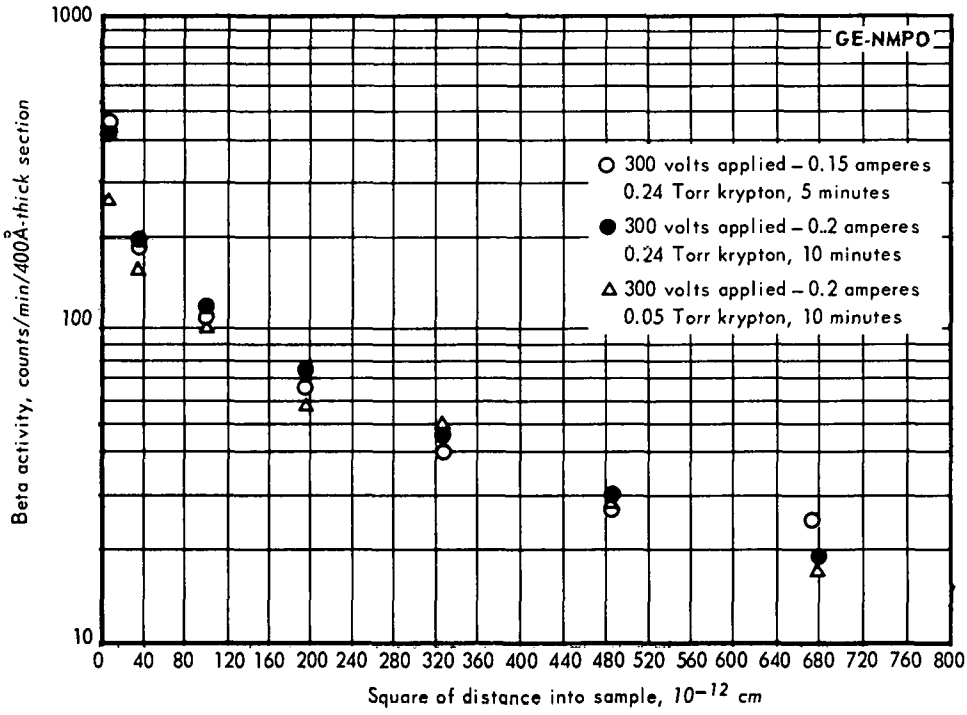

Fig. 3.2 – Distribution of Kr^{85} in arc-cast tantalum sheet samples (~16μ grain size) following absorption and diffusion under glow discharge at 1730°C

of-distance into the sample. These data indicate that beyond approximately 400 Å, diffusion along high diffusivity paths is the dominant transport process under these test conditions. If the concentration in the first section removed ($\sim 10^{-4}$ atom fraction of Kr) does not exceed the solubility limit of the gas in the metal, it is possible that volume diffusion is dominant in the first few hundred angstroms. Other distribution curves are being obtained using 100 Å-thick sections to examine this possibility.

Larger grained (0.5 to 2 mm in diameter) samples were prepared by heat-treating the fine-grained material at 2400°C. The samples were subsequently cooled to 1730°C, subjected to glow discharge for 10 minutes, and then sectioned in 200 Å-thick sections. Even when tested for longer times than the fine-grained samples, these samples exhibited less activity than did the fine-grained samples. Within the data scatter, the distribution of krypton was linear with distance into the sample from the first section, and the slope was in good agreement with those obtained from the fine-grained samples. This suggests that diffusion along high diffusivity paths is also the dominant transport process under these conditions. Additional analyses of data and experiments are underway to check these interpretations.

RARE GAS PERMEATION STUDIES

Two evacuated arc-cast tantalum permeation specimens (Ta-9 and Ta-10) were tested at 2400°C in krypton (1.3×10^{-3} mole fraction Kr^{85}) at a pressure of approximately 625 Torr. One specimen (Ta-9) was tested for 100 hours in two 50-hour increments, and the other (Ta-10) was tested for a single 75-hour period. At the end of the tests, each specimen had a dull, dark gray surface coloration which was identified by X-ray diffraction as alpha - tantalum pentoxide. The source of the oxygen contamination has not yet been identified.

During the second 50-hour increment, specimen Ta-9 was oxidized and permeated by krypton as indicated by a gamma count rate of about 4000 cpm (counter efficiency, ~15%) and a beta count rate of about 300 to 400 cpm (counter efficiency, ~50%); no evidence of krypton penetration into specimen Ta-10 was found even though it too was oxidized. From the count rates on specimen Ta-9, the final krypton pressure in the specimen was calculated to be approximately 7 percent of the pressure outside the sample. A leak-test at room temperature, using helium gas at 7 kg/cm^2, revealed no leaks in the specimen; however, the gamma count rate dropped to zero when the specimen was broken, indicating that the gas was inside the specimen rather than trapped in the oxide. Inspection of the broken pieces revealed that the interior surfaces also had a gray discoloration but that the fractured edges had a metallic appearance. Metallographic mounts are being prepared of the broken pieces for a more detailed visual and electron probe examination. The behavior of specimen Ta-9 is not typical of arc-cast tantalum; several other such specimens have been tested under similar conditions for longer periods of time without evidence of krypton penetration.[3]

TRANSPORT OF FISSION PRODUCTS IN REFRACTORY METALS

Work to determine the migration and release of fission products (other than the rare gases) through refractory metals was continued in two phases: (1) determination of the fission product distribution in refractory metals used to contain fuel during irradiation at high temperature and (2) determination of the extent of release of fission products other than the rare gases by measuring the magnitude of specific fission products deposited on the in-pile test assembly adjacent to the canned sample.

[3] "High-Temperature Materials Program Progress Report No. 46, Part A," GE-NMPO, GEMP-46A, April 15, 1965, p. 12.

Determination of Fission Product Distribution

The fission product distribution in refractory metals used to contain urania fuel during irradiation is being determined by obtaining very small counting samples after grinding away 100- to 250-micron-thick increments of the bottom plate. Both abrasive and anodization - mechanical stripping techniques were demonstrated, in the remote handling cell facilities, for obtaining very small counting samples from an unirradiated tantalum specimen. Measurements are underway in these facilities to calibrate the counting sample size and to determine the reproducibility of removing 100- to 250-micron-thick increments by grinding.

Determination of Fission Product Release

As reported previously,[4] fission products were found in the in-pile test assembly in which a tantalum-canned fuel sample was irradiated for 1035 hours at 1850° to 2000°C. The fission products present on the assembly surfaces were in excess of the release predicted from rare gas release measurements during the test, suggesting that either migration of solid fission products through the metal can was more pronounced than was the migration of rare gases, or that the test assembly was contaminated during the many disassembly operations.

Analysis of the fission product release from a W-Re-Mo-canned fuel sample was begun during this report period. Rare gas release data obtained during the 1015-hour, 2000°C irradiation indicated very little release of fission gases from the metal can. The amount of other fission products (I^{131}, Cs^{137}, Ba^{140}, Sr^{89}, Zr^{95}) were present in the primary experimental capsule in lesser amounts than predicted. Particular care was taken during the dismantling of the capsule to assure the absence of cross contamination. Additional data are being obtained from the exit gas ducting. From these data it appears likely that the earlier determinations of fission product release from Ta-canned fuel was compromised by contamination from other sources.

EFFECT OF FISSION PRODUCTS ON MECHANICAL PROPERTIES

A continuing literature search has thus far revealed very little information regarding the effect of small amounts of substitutional impurities on the high-temperature mechanical properties of refractory metals; however, there is reason to believe that creep resistance may be affected by such impurities. Plans for studying the high-temperature creep characteristics of refractory metals impregnated with fission products at high temperatures were formulated.

Preliminary design studies demonstrated the overall feasibility of in-pile impregnation of refractory-metal specimens with fission products at high temperatures for subsequent mechanical properties testing. Small specimen size is desired in order to impregnate as large a volume fraction of the specimens as possible with recoil fission products since it is not known whether thermal mobility is sufficient to diffuse the recoiled products effectively during the 1800° to 2200°C irradiation. Preliminary study indicates that the specimens should be wire configuration surrounded with a UO_2 sheath designed to act as the in-pile source of heat as well as to provide fission products by recoil. A study of heat transfer and materials compatibility in the irradiation capsule is in progress.

WORK PLANNED FOR NEXT PERIOD

Experimental studies of the movement of krypton through tantalum will continue. Diffusion and permeation studies on tantalum will be expanded to include single crystals and powder metallurgy samples, respectively.

Determination of the distribution of fission products in an irradiated tantalum fuel container will be started and work will be initiated on the fabrication of tungsten creep specimens and components for the in-pile test cartridge.

[4] Ibid.

4. INTERNAL CONVERSION CERAMIC FUEL ELEMENT RESEARCH (57072)

The objectives of this program are to study the chemistry involved in the use of a fertile material (thoria) in stabilized fuel - BeO systems and to develop its capability as an internal conversion fuel element.

EVALUATION OF BeO-BASE FUEL ELEMENTS

Studies were continued on extruded BeO-base fuel elements containing 7 to 25 volume percent UO_2-ThO_2 and UO_2-ThO_2-Y_2O_3 solid solutions. These studies are primarily concerned, at present, with in-pile testing of uncoated fuel elements containing 25 volume percent UO_2-ThO_2-Y_2O_3, and the preparation of BeO-coated fuel elements for future in-pile testing. In addition, bench tests in support of the in-pile tests were continued.

Most of the fuel elements being studied are homogeneously fueled, have a hexagonal external configuration, and a cylindrical bore with nominal sintered dimensions of 0.76 cm across flats and 0.5 cm diameter bores. Fuel elements designated 6BF-243 are tubular with nominal sintered dimensions of 0.7 cm OD and 0.55 cm ID.

Irradiation Testing

Status of the irradiation program is summarized in Table 4.1. The ETR tests are run in sealed capsules; the objective of these static tests is to determine the effect of high fuel burnup on the physical integrity of the fuel elements. The two ETR tests (GEFP2-19 and -23) in progress on uncoated fuel elements have operated satisfactorily for 2500 hours at approximately 1250°C. Non-nuclear bench test specimens being run to duplicate the ETR irradiation time and temperature conditions have shown essentially no change after 1900 hours of testing. The purpose of the ETR test of BeO-coated fuel elements in cartridge GEFP2-22, awaiting insertion, is to assess the capability of the coating to restrict fission product release.

One dynamic test (LTC-73) on uncoated fueled tubes was run in the LITR for 931 hours at temperatures from 1250° to 1550°C to determine the kinetics of fission product re-

TABLE 4.1

IRRADIATION TEST PROGRAM OF BeO FUELED WITH UO_2-ThO_2-Y_2O_3 COMPOSITIONS

Test Number	Specimen Designation[a]	Test Facility	Fuel Composition, mole ratio UO_2	ThO_2	Y_2O_3	Coating	Operating Conditions Time, hr	Temperature, °C	Desired Burnup, 10^{20} fissions/cm^3	Status
GEFP2-19	11.5BF-230	ETR	1	3	0.55	None	2500	1000 - 1250	2 to 5	In progress
GEFP2-22	6BF-243	ETR	1	7	0.55	BeO[b]	-	1250	1 to 2.5	Awaiting insertion
GEFP2-23	11.5BF-230	ETR	1	3	0.55	None	2500	1000 - 1250	1 to 2.5	In progress
LTC-73	11.5BF-230	LITR	1	3	0.55	None	931	1250 - 1550	-[c]	Test complete, evaluation in progress
LTC-74	11.5BF-230	LITR	1	3	0.55	BeO[b]	-	1250 - 1550	-[c]	Awaiting insertion

[a]The first number of the fuel element designation is the UO_2 content of the specimen in weight percent. All fuel elements contain 25 volume percent fuel additive in BeO.

[b]Fuel elements were dip-coated with 0.004 to 0.007 cm of BeO.

[c]Burnup not applicable; this is a dynamic test, the primary purpose of which is to determine fission product release kinetics.

lease. The rare gas analyses obtained during this test indicated recoil fission product release to be the dominant release process.[1] The lack of a diffusion contribution and the lack of any temperature dependence for fission gases released was contrary to previous experience with other fuel compositions. Therefore, the exhaust gas ducting from the test was analyzed by radiochemistry for I^{131}. The fractional release obtained from the ducting ($R/B = 10^{-4}$) was comparable to the values obtained for the rare gases during testing ($R/B = 2$ to 3×10^{-4}) which further supports the interpretation that the dominant release process for this composition is recoil in the temperature range from 1250° to 1550°C. Other post-irradiation evaluations of LTC-73 were reported previously.[2]

A second LITR test (LTC-74) was fabricated and is scheduled for insertion in late May or early June 1965. LTC-74 contains BeO-coated fuel elements which have a composition identical to that of the uncoated LTC-73 fuel elements. The purpose of this test is to determine the ability of BeO to restrict fission product release and corroborate the conclusions derived from LTC-73 since, if recoil is the mechanism of fission product release, the BeO coating should substantially reduce it.

BeO Coating Studies

During this report period, 11.5BF-230 fuel elements (for LTC-74) were coated with BeO following the same procedure used in coating 6BF-243 elements for ETR test GEFP2-22.[3] The matrix and coating were simultaneously densified at 1800°C for 1 hour in H_2. BeO coatings on the 11.5BF-230 tubes differed from those on the 6BF-243 fuel elements in that they were more dense, larger grained, and contained macroscopic fuel particles (see Figure 4.1). These differences in coating structure are attributed to the greater amount of yttrium in the 11.5BF-230 composition (5.3 wt % for 11.5BF-230 vs 2.9 wt % for 6BF-243) which, upon sintering above the $BeO \cdot Y_2O_3$ eutectic temperature of 1580°C, forms a greater amount of liquid eutectic phase.

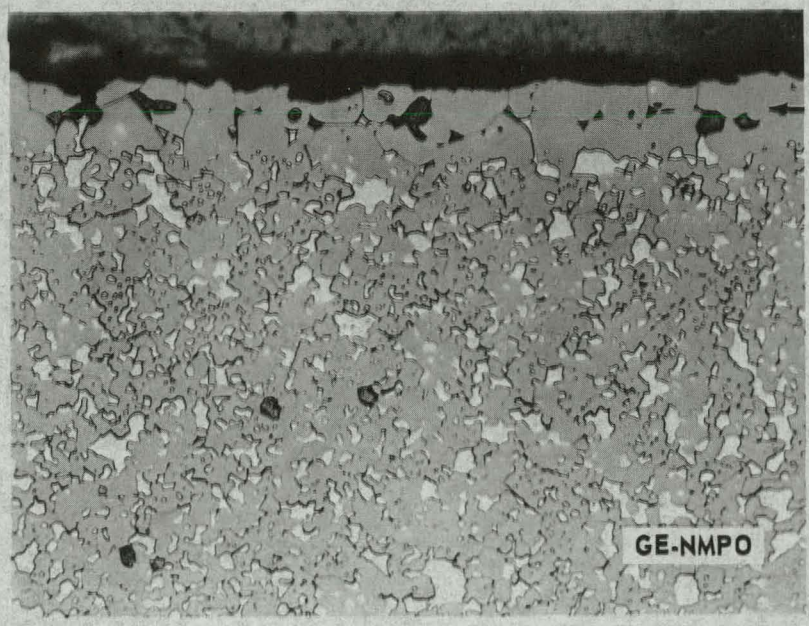

Fig. 4.1 – Microstructure of BeO-coated BeO-base fuel element containing 25 vol. % UO_2-ThO_2-Y_2O_3 *(Neg. 5778, as-sintered, unetched, 250X)*

[1] "Fourth Annual Report – High-Temperature Materials and Reactor Component Development Programs, Volume I – Materials," GE-NMPO, GEMP-334A, February 26, 1965, pp. 196–199.

[2] "High-Temperature Materials Program Progress Report No. 46, Part A," GE-NMPO, GEMP-46A, April 15, 1965, p. 20.

[3] Ibid., pp. 16–18.

In an effort to improve the BeO coating density and to restrict grain growth, 3 weight percent ZrO_2 sol was added to the BeO coating solution. Direct blending of the BeO slip and ZrO_2 sol resulted in a semisolid having undesirable coating properties; therefore, the ZrO_2 sol was first blended with BeO powder, dried, and ignited and then the coating slip was prepared in the usual way. Initial observations of the coatings after sintering at 1800°C indicated that this addition of ZrO_2 did not improve the coating microstructure. Additional specimens will be sintered at lower temperatures in an effort to reduce grain growth and diffusion of fuel into the coating.

Fuel Retention Tests

The results of fuel retention tests of uncoated fuel elements in moving air at 1200°C and 1400°C were presented previously;[4,5] however, the test specimens had not yet been chemically analyzed. Fuel losses calculated from chemical analysis, which were performed during this report period, are listed in Table 4.2 for fuel elements containing 7 to 25 volume percent UO_2-ThO_2-Y_2O_3 solid solutions. These results confirm the previous conclusion that Y_2O_3-containing specimens are superior to non-Y_2O_3-containing specimens (11BF-27) in fuel retention capability. The data illustrate the excellent stability of Y_2O_3-containing fuel elements even under severe test conditions (5000 hours at 1400°C in air).

TABLE 4.2

FUEL LOSS FROM UNCOATED BeO-BASE FUEL ELEMENTS

Fuel Element Designation And UO_2 Content[a]	Fuel Composition, mole ratio			Fuel Content In BeO, vol %	UO_2 Loss[b] After Testing, wt %			
					2000 Hours At 1200°C In		5000 Hours In Air	
	UO_2	ThO_2	Y_2O_3		Helium	He + 5 Vol % O_2	At 1200°C	At 1400°C
11BF-27	1	1	0	7	0.5	1.4	0.6	-
11BF-227	1	1	0.55	11.5	0.3	0.0	0.2	-
7BF-229	1	2	0.55	9.5	0.0	0.0	0.4	-
5BF-230	1	3	0.55	8.5	0.0	0.0	0.0	-
11.5BF-230	1	3	0.55	25	0.0	0.0	0.2	0.3

[a]The first number of the fuel element designation is the UO_2 content of the specimen in weight percent.
[b]UO_2 loss was calculated from the difference in chemical analysis of specimens before and after testing. Values are the average of two specimens sintered at either 1675°C for 2 hours or 1800°C for 1 hour in hydrogen having a dewpoint of 0°C.

WORK PLANNED FOR NEXT PERIOD

Irradiation testing will be continued in the ETR on BeO-base fuel elements containing 25 volume percent of a UO_2-ThO_2-Y_2O_3 solid solution. A third ETR test (GEFP2-22) of high-ThO_2-content fuel elements coated with BeO is scheduled for insertion in May 1965. A second LITR test (LTC-74) using BeO-coated fuel elements, is scheduled for insertion in late May or early June 1965. Non-nuclear bench testing of specimens to duplicate the irradiation test conditions will continue together with limited coating studies. Post-irradiation examinations will be continued on LTC-73.

[4]Ibid., pp. 15–16.

[5]"Fourth Annual Report – High-Temperature Materials and Reactor Component Development Programs, Volume I – Materials," GE-NMPO, GEMP-334A, February 26, 1965, pp. 192–196.

5. RADIATION EFFECTS IN BeO

(57063)

The purpose of this program is to define the irradiation behavior of BeO in terms of the composition and microstructure variables that contribute to extended radiation stability.

IRRADIATION STATUS

A summary of the current series of irradiation tests is given in Table 5.1. The 100°C tests completed previously have been returned to GE-NMPO for disassembly and post-test examination. Operation of the size-effect and thermal conductivity test, GEFP2-134, began during this report period. The thermocouples pertinent to the thermal conductivity measurements failed early in the test and it will not be possible to obtain these data. Exposure of the samples, which are approximately 2.5 cm in diameter and length, is continuing at 900°C, the maximum temperature that could be attained. Test capsule GEFP2-132, in which previously irradiated samples will be further irradiated, is at the ETR for insertion during the June shutdown. Test GEFP2-135, to determine in-pile annealing of previously induced defects, remains tentative; the earliest practicable insertion date appears to be late summer.

TABLE 5.1

PLANNED IRRADIATION TESTS OF BeO

Test Number	Irradiation Conditions: Temperature, °C	Irradiation Conditions: Dosage, 10^{20} nvt (≥1 Mev)	Purpose	Approximate Irradiation Dates: Start	Approximate Irradiation Dates: End
GEFP2-216, GEFP2-217	100	1 to 2	Evaluation of BeO + Be and Thermalox 995 compositions	1/1/65	3/31/65
GEFP2-223, GEFP2-226	100	2 to 5			
GEFP2-134	1000	10 to 20	Size effect and relative thermal conductivity	3/29/65	2/66
GEFP2-132	1000	20 to 40[a]	Determine if saturation of expansion occurs	6/15/65	1/15/66
GEFP2-135	1200	2 to 4[a]	Determine in-pile annealing of previously induced defects	Tentative	

[a]Figures shown are dosages to be added in this irradiation. These specimens have accumulated dosages of 2 to 6 x 10^{21} nvt (≥ 1 Mev) at about 1000°C in previous irradiations.

PROPERTIES OF UNIRRADIATED BeO

Efforts have been in progress for some time to obtain relatively accurate measurements of the bulk and apparent volumes and densities of the specimens as a means of supplementing dimensional measurements and of obtaining open and closed porosity data. The commonly used procedures for such measurements are of the type described in ASTM method C 20-46, in which the desired information is obtained from specimen weight in the dry condition, impregnated with water, and submerged in water. (Definition

of the terminology of the volume and density measurements is given in Table 5.2.) The accuracy of the bulk volume measurements in this procedure is limited by the method of determining the weight of the specimen impregnated with water; both the blotting operation to remove excess water and evaporation of the water from the impregnated specimen during weighing lead to errors. Evaluation of a number of alternate fluids as well as various modifications of the procedure lead to the use of diethylphthalate for the bulk volume measurement. With this fluid, a bulk volume of 1 cm^3 could be reproduced within 0.1 percent. However, the fluid penetrates into the open pores somewhat slowly; therefore, a different fluid that would penetrate more rapidly was desirable for the apparent volume measurement to reduce the time required for completing both bulk and apparent volume measurements.

TABLE 5.2

DEFINITION OF TERMINOLOGY OF VOLUME AND DENSITY MEASUREMENTS FOR UNIRRADIATED BeO

Bulk volume = volume of specimen including the volume of the open and closed pores
$\text{Bulk volume} = \frac{\text{saturated weight - suspended weight}}{\text{density of suspension liquid}}$
$\text{Bulk density} = \frac{\text{dry weight}}{\text{bulk volume}}$
Apparent volume = volume of specimen exclusive of the volume of open pores
$\text{Apparent volume} = \frac{\text{dry weight - suspended weight}}{\text{density of suspension liquid}}$
$\text{Percent total porosity} = \frac{\text{theoretical density - bulk density}}{\text{theoretical density}} \times 100$
$\text{Percent open porosity} = \frac{\text{apparent density - bulk density}}{\text{apparent density}} \times 100$

In the improved procedure, toluene is used as the impregnating and weighing fluid to determine the apparent volume. Other fluids, i.e., water and heavy liquids such as carbon tetrachloride and trichloroethylene, are equally satisfactory for determining apparent volume; however, toluene appears to penetrate the pores somewhat faster than water and temperature control is more easily maintained than with the heavy liquids. Overnight soaking following vacuum impregnation is adequate for the toluene to penetrate the pores of all specimens except those with greater than 10 percent open porosity which required 3 to 5 days. Toluene is removed from the specimens by overnight exposure in a drying oven.

Diethylphthalate is used solely to determine the bulk volume. To avoid the time lapse required for complete impregnation, the volume is determined from the impregnated weight and weight submerged in the liquid;[1] this method also provides apparent volume data which can be compared to the toluene values. Samples are vacuum impregnated and are allowed to soak overnight. For most samples, this treatment gives adequate impregnation; however, for specimens of high open porosity, a longer soak period may be necessary to avoid weight changes between the two weighings. The blotting operation preparatory to obtaining the impregnated weight does not appear particularly critical. Specimens taken from the liquid are first blotted on paper towels thoroughly soaked with the diethylphthalate, then blotted on a smooth-finish bond paper sheet, one half wetted

[1]Determination of the open porosity from the difference between the impregnated and dry weights requires complete impregnation.

with the diethylphthalate and the other half dry. Blotting proceeds from the wetted end to the dry end of the paper. With this procedure an impregnated weight of 3.5 grams can be reproduced within 1 milligram by different operators. The diethylphthalate can usually be removed by boiling 2 to 4 hours in trichloroethylene; however, heating at about 500°C may be required for specimens with greater than 10 percent open porosity.

A comparison of the density and porosity data obtained with toluene - diethylphthalate (T-D) versus those obtained with water (plus 0.1% wetting agent) is given in Table 5.3. The values are recorded in the sequence in which the measurements were made, i.e., in T-D, in water after 7 days soaking, in water after 21 days soaking, then in T-D. The data show that the T-D measurements yield values comparable to those obtained with water. The apparent density and total porosity values should, and do, agree quite well. The bulk density and open porosity values differ to some extent, principally because of the relatively poor reproducibility of the impregnated weights using water. Little credence is attached to these water values other than as an indication of the magnitude of the open porosity. Because of the significantly better reproducibility of the bulk volume measurements, the T-D data are probably the more accurate; mercury intrusion data are being obtained for further comparison.

Density and Porosity Data on BeO Specimens

Using the procedure described in the preceding paragraphs, measurements of the total and open porosity were completed on representative samples of each of the compositions, grain sizes, and densities used in the irradiation studies. In most instances, specimens of a given grain size and density were obtained from four different sintering batches prepared at different times. With the exception of a few isostatically pressed materials, the specimens were prepared by extrusion and in all cases sintered in hydrogen. All specimens had been centerless ground to final dimensions of 0.604 ± 0.0025 cm diameter and, in many instances, duplicate specimens of 4.37 cm length were obtained by cutting specimens originally 8.9 cm long in half.

The density and porosity data are given in Table 5.4. In general, the data for two specimens fabricated from the same piece are in excellent agreement, indicating longitudinal uniformity of the specimens. The poorest samples in this respect include some of the lowest density specimens, in which some variation of the open and closed porosity is probably to be expected, and some of the compositions containing glass-phase additives. These latter materials were prepared in only one or two batches and it is doubtful that the results cited here are representative of the uniformity that might be obtained with further experience in handling and sintering. Interestingly, the open porosity in the majority of the compositions and grain sizes was less than 1 percent even when the total porosity was as much as 10 to 15 percent. Open porosity is appreciable only in specimens with bulk densities less than 2.7 g/cm^3 and varies from low to high values in this group. In this respect, the specimens appear to differ appreciably from the cold-pressed - sintered and hot-pressed specimens described by Ross.[2] The comparison with Ross' data is illustrated in Figure 5.1. The data points in the figure are for materials of approximately 5-micron grain size but the data are representative of larger grain sizes. The cause of the difference in open porosity is not known; in addition to the different preparation methods, the starting materials, the sintering atmosphere, and the sintering temperature may be factors.

[2]A. M. Ross, "Penetration Rates of Water into High Density Beryllium Oxide During Vacuum Impregnation at Room Temperature," AERE-R 4783.

TABLE 5.3

COMPARISON OF DENSITY - POROSITY DATA ON BeO SPECIMENS FROM MEASUREMENTS IN WATER AND IN TOLUENE - DIETHYLPHTHALATE

Specimen Description			Apparent Density, g/cm³[a,b]				Bulk Density, g/cm³[a,b]				Total Porosity, percent[a,b]				Open Porosity, percent[a,b]			
Composition	Grain Size, *microns*	Nominal Density, g/cm³	Toluene	Water + 0.1% Calgonite	Water + 0.1% Calgonite	Toluene	Diethyl-phthalate	Water + 0.1% Calgonite	Water + 0.1% Calgonite	Diethyl-phthalate	Toluene - Diethyl-phthalate	Water + 0.1% Calgonite	Water + 0.1% Calgonite	Toluene - Diethyl-phthalate	Toluene - Diethyl-phthalate	Water + 0.1% Calgonite	Water + 0.1% Calgonite	Toluene - Diethyl-phthalate
UOX + 0.5 wt % MgO	5	2.60	2.6518	2.6513	2.6534	2.6515	2.6462	2.6458	2.6462	2.6457	12.08	12.10	12.09	12.10	0.21	0.21	0.27	0.22
		2.75	2.7175	2.7160	2.7165	2.7170	2.7124	2.7123	2.7146	2.7127	9.89	9.89	9.81	9.88	0.19	0.14	0.07	0.16
		2.90	2.9110	2.9105	2.9104	2.9115	2.9088	2.9102	2.9095	2.9081	3.36	3.31	3.34	3.38	0.08	0.01	0.03	0.12
	10	2.60	2.6607	2.6587	2.6591	2.6587	2.6537	2.6557	2.6540	2.6531	11.84	11.77	11.82	11.86	0.26	0.11	0.19	0.21
AOX	5	2.60	2.9987	2.9957	2.9928	2.9921	2.6006	2.5995	2.6001	2.6014	13.60	13.64	13.62	13.57	13.27	13.23	13.12	13.06
		2.75	2.8927	2.8983	2.8990	2.8974	2.7276	2.7308	2.7288	2.7296	9.38	9.27	9.34	9.31	5.71	5.78	5.87	5.78
		2.90	2.9148	2.9121	2.9129	2.9142	2.9104	2.9094	2.9127	2.9103	3.31	3.34	3.23	3.31	0.15	0.10	0.01	0.13
	10	2.75	2.7691	2.7673	2.7669	2.7670	2.7616	2.7603	2.7611	2.7624	8.25	8.30	8.27	8.22	0.27	0.26	0.21	0.16
		2.90	2.8869	2.8874	2.8880	2.8889	2.8843	2.8819	2.8841	2.8845	4.16	4.26	4.18	4.17	0.07	0.19	0.14	0.15
	20	2.60	2.5659	2.5733	2.6151	2.5916	2.5476	2.5444	2.5469	2.5453	15.36	15.47	15.38	15.44	0.71	1.12	2.61	1.79[c]
		2.75	2.7468	2.7503	2.7634	2.7635	2.7383	2.7345	2.7334	2.7366	9.01	9.15	9.19	9.08	0.29	0.57	1.08	0.97[c]
		2.90	2.8896	2.8882	2.8878	2.8894	2.8879	2.8859	2.8869	2.8854	4.06	4.12	4.29	4.14	0.06	0.08	0.24	0.14
	50	2.60	2.6779	2.6758	2.6803	2.6786	2.6672	2.6684	2.6660	2.6649	11.39	11.35	11.43	11.46	0.40	0.28	0.53	0.51
		2.75	2.7704	2.7708	2.7723	2.7725	2.7658	2.7666	2.7646	2.7637	8.11	8.09	8.15	8.18	0.17	0.15	0.28	0.32
		2.90	2.9444	2.9436	2.9437	2.9444	2.9398	2.9410	2.9423	2.9393	2.33	2.29	2.25	2.35	0.16	0.09	0.05	0.18
	80	2.75	2.7469	2.7465	2.7474	2.7469	2.7372	2.7345	2.7356	2.7358	9.06	9.15	9.12	9.11	0.35	0.44	0.43	0.41
		2.90	2.9399	2.9385	2.9377	2.9392	2.9379	2.9355	2.9337	2.9343	2.40	2.48	2.53	2.52	0.07	0.10	0.14	0.17

[a]Values are reported horizontally in the sequence in which the measurements were made. The first-listed values in water were obtained after vacuum impregnation for 7 days; the second-listed values in water were obtained after impregnation for a total of 21 days. The values in the final column were obtained in toluene - diethylphthalate following the measurements in water.

[b]For comparison purposes, all experimental values are cited to one significant figure more than is warranted by reproducibility.

[c]The data for these samples are possibly indicative of changes in the specimens during the measurements; the possibility of reaction with water is being checked in further measurements.

TABLE 5.4

DENSITY AND POROSITY DATA FOR UNIRRADIATED BeO SPECIMENS OF DIFFERENT GRAIN SIZES AND COMPOSITIONS

Specimen Description		Bulk Density,[a,b] g/cm^3	Apparent Density,[c] g/cm^3	Total Porosity,[d] percent	Open Porosity,[d] percent
Composition	Nominal Grain Size, microns				
UOX+0.5 wt % MgO	5	2.578	2.584	14.346	0.210
		2.479	2.971	17.627	16.536
		2.453	2.990	18.500	17.953
		2.641	2.646	12.266	0.196
		2.646	2.652	12.083	0.207
		2.607	2.642	13.393	1.336
		2.588	2.682	14.028	3.521
		2.612	2.620	13.228	0.296
		2.609	2.617	13.321	0.319
		2.712	2.718	9.889	0.192
		2.723	2.728	9.527	0.168
		2.766	2.771	8.107	0.166
		2.769	2.776	8.005	0.181
		2.765	2.773	8.137	0.268
		2.769	2.773	8.003	0.138
		2.749	2.756	8.670	0.243
		2.768	2.776	8.038	0.287
		2.813	2.818	6.558	0.177
		2.811	2.817	6.598	0.184
		2.767	2.771	8.089	0.165
		2.772	2.775	7.894	0.112
		2.909	2.911	3.362	0.076
		2.910	2.912	3.325	0.070
		2.905	2.918	3.480	0.433
		2.904	2.908	3.521	0.148
		2.910	2.914	3.315	0.121
		2.919	2.923	3.017	0.129
		2.918	2.925	3.047	0.222
		2.918	2.922	3.060	0.149
		2.922	2.926	2.940	0.147
		2.906	2.911	3.443	0.148
		2.903	2.906	3.548	0.102
UOX+0.5 wt % MgO	10	2.654	2.660	11.838	0.233
		2.651	2.664	11.914	0.489
		2.656	2.663	11.796	0.298
		2.658	2.667	11.693	0.353
		2.657	2.662	11.726	0.204
		2.657	2.664	11.715	0.241
		2.658	2.664	11.680	0.279
		2.654	2.661	11.836	0.269
		2.780	2.784	7.629	0.137
		2.775	2.781	7.809	0.213
		2.776	2.783	7.779	0.260
		2.770	2.774	7.984	0.167
		2.779	2.781	7.814	0.210
		2.762	2.769	8.227	0.223
		2.784	2.789	7.514	0.173
		2.778	2.784	7.697	0.191
		2.881	2.884	4.276	0.107
		2.881	2.883	4.270	0.037
		2.932	2.940	9.924	0.289
		2.913	2.921	3.209	0.242
		2.911	2.916	3.291	0.182
		2.951	2.955	1.948	0.134
		2.952	2.954	1.919	0.079
		2.932	2.936	2.606	0.146
UOX+0.5 wt % MgO	20	2.614	2.621	13.154	0.249
		2.614	2.622	13.170	0.331
		2.623	2.629	12.866	0.234
		2.621	2.628	12.913	0.298
		2.604	2.611	13.500	0.298
		2.611	2.618	13.271	0.296
		2.625	2.633	12.804	0.319
		2.626	2.632	12.745	0.210
		2.745	2.751	8.793	0.216
		2.743	2.750	8.858	0.244
		2.751	2.760	8.530	0.291
		2.781	2.787	7.609	0.227
		2.782	2.785	7.587	0.129
		2.750	2.757	8.622	0.224
		2.750	2.757	8.648	0.248
		2.880	2.884	4.306	0.182
		2.884	2.889	4.181	0.185
		2.907	2.911	3.424	0.151
		2.910	2.915	3.334	0.180
		2.900	2.904	3.661	0.139
		2.902	2.907	3.599	0.175
		2.911	2.918	3.296	0.253
		2.912	2.917	3.264	0.149

TABLE 5.4 (Cont.)

DENSITY AND POROSITY DATA FOR UNIRRADIATED BeO SPECIMENS OF DIFFERENT GRAIN SIZES AND COMPOSITIONS

Specimen Description					
Composition	Nominal Grain Size, microns	Bulk Density,[a,b] g/cm³	Apparent Density,[c] g/cm³	Total Porosity,[d] percent	Open Porosity,[d] percent
UOX+0.5 wt % MgO (Isostatically pressed)	20	2.956	2.957	1.796	0.045
		2.951	2.957	1.962	0.190
		2.952	2.957	1.916	0.159
		2.955	2.959	1.841	0.150
		2.955	2.960	1.812	0.152
		2.956	2.958	1.794	0.053
UOX+0.5 wt % MgO	50	2.649	2.662	11.980	0.460
		2.648	2.660	12.040	0.471
		2.644	2.656	12.147	0.443
		2.652	2.648	12.550	0.981
		2.683	2.691	10.880	0.324
		2.683	2.693	10.880	0.404
		2.690	2.698	10.627	0.297
		2.686	2.693	10.755	0.241
		2.723	2.824	9.529	3.578
		2.721	2.808	9.600	3.114
		2.764	2.777	8.176	0.457
		2.767	2.777	8.071	0.350
		2.751	2.766	8.610	0.539
		2.748	2.766	8.707	0.668
		2.763	2.774	8.203	0.390
		2.766	2.777	8.122	0.410
		2.948	2.980	2.048	0.087
		2.948	2.980	2.073	0.098
		2.904	2.909	3.821	0.148
		2.901	2.907	3.808	0.207
		2.899	2.904	3.681	0.165
		2.895	2.901	3.836	0.214
		2.884	2.889	4.197	0.184
		2.885	2.891	4.144	0.185
UOX+0.5 wt % MgO	80	2.807	2.816	6.790	0.328
		2.803	2.816	6.864	0.463
		2.831	2.837	5.488	0.230
		2.830	2.837	5.983	0.256
		2.748	2.761	8.498	0.466
		2.757	2.766	8.481	0.386
		2.794	2.775	8.501	0.755
		2.782	2.780	8.582	1.018
		2.895	2.900	3.827	0.172
		2.895	2.899	3.807	0.136
		2.932	2.936	2.608	0.127
		2.933	2.936	2.571	0.108
		2.920	2.926	2.994	0.212
		2.917	2.922	3.101	0.196
		2.913	2.918	3.230	0.188
		2.911	2.917	3.286	0.217
UOX+0.5 wt % MgO	100	2.964	2.967	1.831	0.097
		2.964	2.967	1.828	0.098
		2.950	2.954	2.003	0.131
		2.948	2.955	2.087	0.233
		2.915	2.918	3.169	0.101
		2.918	2.923	3.058	0.171
		2.922	2.929	2.924	0.245
		2.920	2.924	2.975	0.134
AOX	5	2.574	2.579	14.498	0.227
		2.575	2.582	14.448	0.247
		2.601	2.999	13.600	13.275
		2.601	2.999	13.579	13.249
		2.553	2.583	15.171	1.161
		2.597	2.610	13.721	0.505
		2.718	2.954	9.704	7.998
		2.730	2.927	9.296	6.714
		2.727	2.893	9.387	5.714
		2.751	2.759	8.591	0.279
		2.800	2.803	6.972	0.089
		2.797	2.800	7.067	0.094
		2.800	2.805	6.962	0.156
		2.802	2.809	6.920	0.275
		2.733	2.775	9.186	1.504
		2.726	2.782	9.450	2.028
		2.762	2.772	8.228	0.345
		2.754	2.767	8.497	0.451
		2.762	2.771	8.225	0.309
		2.586	2.762	14.072	6.356
		2.904	2.917	3.525	0.445
		2.911	2.915	3.303	0.146
		2.907	2.912	3.434	0.189
		2.910	2.916	3.320	0.194
		2.919	2.922	3.039	0.135
		2.893	2.899	3.878	0.191

TABLE 5.4 (Cont.)

DENSITY AND POROSITY DATA FOR UNIRRADIATED BeO SPECIMENS OF DIFFERENT GRAIN SIZES AND COMPOSITIONS

Specimen Description		Bulk Density,[a, b] g/cm^3	Apparent Density,[c] g/cm^3	Total Porosity,[d] percent	Open Porosity,[d] percent
Composition	Nominal Grain Size, microns				
AOX	5	2.917	2.921	3.106	0.146
		2.916	2.921	3.138	0.175
	10	2.641	2.646	12.262	0.197
		2.643	2.647	12.188	0.159
		2.644	2.651	12.162	0.248
		2.645	2.652	12.129	0.253
		2.619	2.626	13.004	0.266
		2.620	2.628	12.948	0.284
		2.638	2.645	12.348	0.250
		2.640	2.647	12.305	0.262
		2.764	2.770	8.171	0.215
		2.765	2.771	8.133	0.216
		2.764	2.772	8.197	0.274
		2.763	2.773	8.213	0.374
		2.761	2.769	8.291	0.277
		2.758	2.766	8.378	0.283
		2.782	2.786	7.691	0.151
		2.794	2.798	7.177	0.163
		2.885	2.887	4.163	0.078
		2.885	2.888	4.180	0.141
		2.869	2.870	4.674	0.028
		2.872	2.876	4.595	0.118
		2.893	2.896	3.903	0.130
		2.888	2.893	4.039	0.173
		2.858	2.863	5.042	0.156
		2.860	2.864	4.996	0.136
AOX	20	2.664	2.672	11.490	0.306
		2.662	2.669	11.563	0.270
		2.547	2.563	18.384	0.629
		2.547	2.566	18.367	0.721
		2.583	2.609	14.847	1.759
		2.580	2.602	14.946	1.698
		2.595	2.628	13.773	1.119
		2.594	2.622	13.806	1.084
		2.739	2.747	9.014	0.297
		2.737	2.746	9.067	0.307
		2.740	2.750	8.987	0.364
		2.740	2.751	8.974	0.388
		2.750	2.757	8.637	0.249
		2.744	2.750	8.880	0.232
		2.770	2.779	7.968	0.319
		2.769	2.779	8.008	0.342
		2.892	2.898	3.929	0.123
		2.894	2.897	3.850	0.101
		2.874	2.878	4.521	0.138
		2.878	2.881	4.384	0.089
		2.888	2.890	4.057	0.062
		2.885	2.888	4.168	0.123
		2.888	2.890	4.165	0.195
		2.890	2.898	4.001	0.245
		2.906	2.908	3.467	0.072
AOX (Isostatically pressed)	20	2.906	2.910	3.458	0.127
		2.949	2.954	2.022	0.165
		2.947	2.951	2.099	0.152
		2.944	2.949	2.208	0.193
		2.945	2.948	2.168	0.126
		2.944	2.948	2.194	0.147
		2.945	2.949	2.213	0.190
		2.949	2.953	2.032	0.140
		2.946	2.951	2.114	0.166
AOX	50	2.655	2.665	11.806	0.402
		2.653	2.664	11.856	0.406
		2.667	2.678	11.384	0.396
		2.674	2.686	11.155	0.442
		2.766	2.770	8.116	0.170
		2.765	2.771	8.147	0.227
		2.761	2.769	8.282	0.317
		2.761	2.770	8.258	0.297
		2.959	2.962	1.707	0.126
		2.960	2.963	1.650	0.083
		2.931	2.938	2.619	0.217
		2.940	2.944	2.336	0.161
		2.937	2.943	2.420	0.189
		2.620	2.628	12.964	0.300
		2.622	2.628	12.892	0.221
AOX	80	2.737	2.747	9.060	0.350
		2.738	2.746	9.051	0.293
		2.781	2.791	7.593	0.340
		2.779	2.786	7.678	0.268
		2.937	2.941	2.414	0.123
		2.938	2.940	2.395	0.068

TABLE 5 4 (Cont.)

DENSITY AND POROSITY DATA FOR UNIRRADIATED BeO SPECIMENS OF DIFFERENT GRAIN SIZES AND COMPOSITIONS

Specimen Description					
Composition	Nominal Grain Size, microns	Bulk Density,[a,b] g/cm^3	Apparent Density,[c] g/cm^3	Total Porosity,[d] percent	Open Porosity,[d] percent
AOX	80	2.949	2.952	2.041	0.118
		2.951	2.952	1.959	0.049
	100	2.966	2.977	1.455	0.370
		2.966	2.977	1.447	0.366
		2.955	2.961	1.837	0.224
HPA[e]	5	2.955	2.965	1.813	0.313
		2.709	2.813	9.988	3.669
HPA[e]	20	2.710	2.816	9.955	3.747
		2.890	2.895	3.988	0.183
		2.894	2.898	3.862	0.154
HPA[e]	50	2.908	2.915	3.373	0.221
		2.907	2.913	3.429	0.208
		2.919	2.924	3.010	0.159
		2.930	2.935	2.667	0.180
		2.877	2.882	4.435	0.176
		2.880	2.883	4.323	0.117
		2.932	2.940	2.582	0.259
		2.943	2.945	2.213	0.072
		2.916	2.922	3.109	0.199
		2.940	2.944	2.324	0.121
HPA[e]	80	2.918	2.924	3.040	0.200
		2.946	2.949	2.131	0.110
		2.961	2.966	1.611	0.155
		2.961	2.962	1.638	0.058
		2.922	2.928	2.924	0.204
		2.942	2.947	2.261	0.166
		2.921	2.928	2.954	0.242
		2.917	2.920	3.094	0.111
		2.892	2.899	3.924	0.260
		2.894	2.903	3.840	0.282
UOX	5	2.896	2.900	3.799	0.166
		2.887	2.891	4.090	0.129
		2.885	2.890	4.141	0.177
		2.883	2.887	4.218	0.126
		2.920	2.931	2.976	0.346
UOX	20	2.882	2.891	4.261	0.337
		2.908	2.913	3.400	0.188
		2.899	2.903	3.686	0.122
		2.897	2.904	3.750	0.248
		2.886	2.890	4.131	0.167
		2.877	2.882	4.407	0.165
		2.883	2.887	4.204	0.140
UOX (Isostatically pressed)	20	2.886	2.890	4.104	0.121
		2.935	2.941	2.486	0.187
		2.938	2.940	2.397	0.071
UOX	30	2.923	2.929	2.883	0.193
		2.924	2.929	2.865	0.191
		2.962	2.966	1.583	0.118
		2.966	2.968	1.452	0.047
UOX+3 wt % ZrO_2	5	2.924	2.931	3.965[f]	0.218
UOX+3 wt % ZrO_2	20	2.938	2.943	3.872[f]	0.141
		2.981	2.988	2.097[f]	0.237
		2.986	2.988	2.097[f]	0.064
		2.919	2.925	4.161[f]	0.225
		2.896	2.903	4.915[f]	0.260
		2.907	2.912	4.587[f]	0.169
		2.919	2.924	4.194[f]	0.177
		2.928	2.932	3.932[f]	0.153
		2.914	2.919	4.358[f]	0.150
		2.936	2.941	3.637[f]	0.159
		2.941	2.942	3.604[f]	0.052
		2.949	2.952	3.277[f]	0.126
		2.949	2.953	3.244[f]	0.133
		2.988	3.017	1.147[f]	0.944
		2.986	2.989	2.064[f]	0.100
		2.979	2.987	2.130[f]	0.293
		2.985	2.989	2.064[f]	0.142
		3.031	3.034	0.590[f]	0.091
		3.026	3.034	0.590[f]	0.253
		3.034	3.036	0.524[f]	0.080
		3.032	3.037	0.492[f]	0.143
		3.026	3.031	0.688[f]	0.166
		3.026	3.032	0.656[f]	0.166
		3.020	3.024	0.918[f]	0.144
		3.020	3.025	0.885[f]	0.161
HPA+0.5 wt % MgO[e]	20	2.885	2.890	4.139	0.164
		2.886	2.891	4.134	0.175
		2.864	2.868	4.854	0.142
		2.865	2.869	4.803	0.114

TABLE 5.4 (Cont.)

DENSITY AND POROSITY DATA FOR UNIRRADIATED BeO SPECIMENS OF DIFFERENT GRAIN SIZES AND COMPOSITIONS

Specimen Description					
Composition	Nominal Grain Size, *microns*	Bulk Density,[a,b] g/cm^3	Apparent Density,[c] g/cm^3	Total Porosity,[d] *percent*	Open Porosity,[d] *percent*
HPA + 0.5 wt % MgO[e]	20	2.860	2.867	4.971	0.235
		2.862	2.864	4.909	0.072
		2.857	2.861	5.091	0.156
EBOR	25	2.858	2.861	5.059	0.122
		2.813	2.819	6.555	0.218
		2.805	2.813	6.796	0.260
		2.813	2.818	6.553	0.201
		2.803	2.807	6.892	0.171
		2.806	2.811	6.768	0.166
		2.793	2.797	7.206	0.129
		2.793	2.798	7.211	0.167
		2.795	2.801	7.159	0.224
		2.775	2.805	7.814	1.082
		2.823	2.829	6.200	0.192
		2.795	2.798	7.136	0.112
		2.792	2.795	7.240	0.108
		2.771	2.777	7.945	0.232
UOX + 1 wt % Bentonite	5	2.830	2.838	5.983	0.291
		2.590	3.003	13.955	13.760
UOX + 1 wt % Bentonite	20	2.621	3.000	12.916	12.627
		2.877	2.882	4.433	0.199
		2.874	2.879	4.505	0.155
UOX + 2 wt % Bentonite	5	2.729	2.734	9.342	0.183
		2.675	2.826	11.134	5.339
UOX + 2 wt % high silica glass	20	2.876	2.880	4.457	0.159
		2.879	2.882	4.367	0.106
		2.877	2.885	4.428	0.276
		2.876	2.884	4.460	0.279
		2.878	2.884	4.384	0.214
		2.878	2.886	4.378	0.284
UOX + 2 wt % Bentonite	20	2.845	2.853	5.467	0.260
		2.850	2.855	5.310	0.167
		2.865	2.870	4.833	0.191
		2.866	2.869	4.773	0.104
		2.728	2.735	9.364	0.239
		2.755	2.761	8.483	0.222
UOX + 2 wt % low silica glass	5	2.882	2.883	4.241	0.020
UOX + 2 wt % medium silica glass	5	2.887	2.892	4.085	0.156
		2.909	2.916	3.361	0.251
UOX + 2 wt % high silica glass	20	2.919	2.921	3.033	0.071
		2.919	2.923	3.025	0.146
		2.922	2.926	2.934	0.141
		2.830	2.836	5.994	0.244
UOX + 1 wt % Al_2O_3		2.832	2.840	5.897	0.269
		2.968	2.973	1.411	0.185
		2.957	2.962	1.767	0.179
HPA (Hot pressed)		2.862	2.960	4.925	3.329

[a] Bulk densities measured with diethylphthalate.
[b] Braces indicate half specimens cut from 8.9-cm-long specimen.
[c] Apparent densities measured with toluene.
[d] Total porosity and open porosity values are significant to only one decimal place.
[e] HPA specimens made from Minox AAA grade of BeO, Mineral Concentrate Co.
[f] Data changed because all calculations on run-off were based on a theoretical density of 3.010 g/cm^3; the theoretical density for UOX + 3 wt % ZrO_2 is 3.052 g/cm^3.

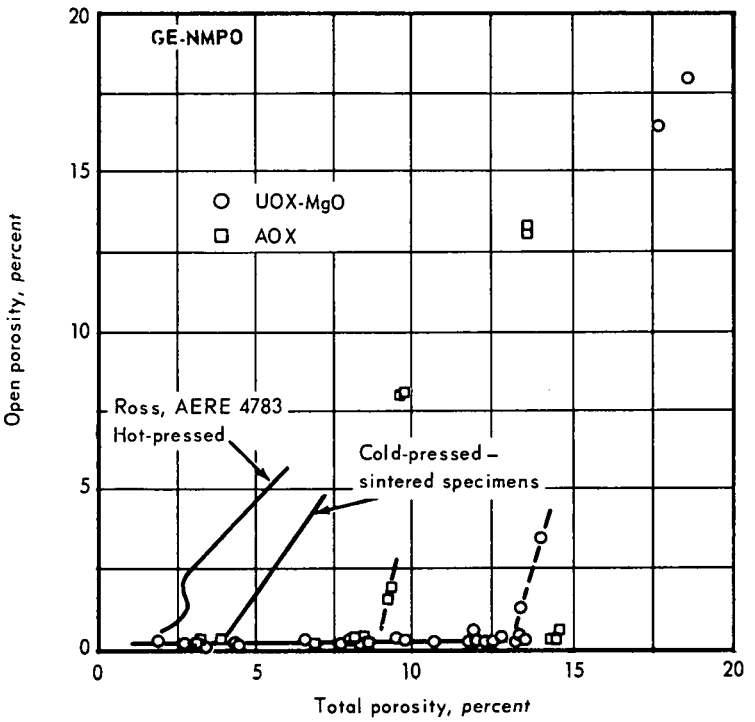

Fig. 5.1 – Open versus total porosity in unirradiated specimens fabricated by extrusion and sintering in hydrogen

Thermal Conductivity

Test runs using the laser thermal diffusivity equipment were completed on Armco iron specimens over the temperature range from 175° to 800°C to check out the equipment. Good agreement was obtained with published values of the resistivity of this material. The first runs on unirradiated BeO specimens will begin following extension of the Armco iron measurements to 1000°C.

MEASUREMENTS OF IRRADIATED BeO

Several post-irradiation measurements were completed on specimens in the second of the two irradiation cartridges in test 33MT105. The objective of this test was to compare the elevated-temperature irradiation behavior of compositions containing glass-phase additives with those of UOX-MgO- and AOX-grade BeO materials. Specimens included the EBOR composition (with 1 wt % bentonite), and compositions containing 1 weight percent high-, medium-, and low-silica content glasses,[3] and 2 weight percent bentonite in UOX-grade BeO. Also included were small grain size specimens containing 1 weight percent Al_2O_3, and 3 weight percent ZrO_2 in UOX. The exposure was to dosages of approximately 10^{21} nvt ($\geq$ 1 Mev) at 1000°C nominally; specimens near the end of the cartridge, i. e., those with the lowest dosages, ran at 900° to 950°C.

Changes in the dimensions, open porosity, and elastic constants are summarized in Table 5. 5. Dimensional changes ranged from 1 to 3 percent, the smallest changes occurring in the 5-micron grain size UOX-MgO specimens of approximately 2.9 g/cm^3. Slightly larger but comparable expansion occurred in the small grain size UOX-MgO,

[3] "Fourth Annual Report – High-Temperature Materials and Reactor Component Development Programs, Volume I – Materials," GE-NMPO, GEMP-334A, February 26, 1965, Table 3.2, p. 124.

TABLE 5.5

DIMENSION AND PROPERTY CHANGES IN BeO SPECIMENS OF SEVERAL COMPOSITIONS IRRADIATED AT 900° TO 1000°C

Specimen Description			Irradiation Conditions						Plastic Constants						
					Expansion, %			Increase in Open Porosity, %	Young's Modulus			Shear Modulus			Poisson's Ratio
Composition	Grain Size, microns	Nominal Density, g/cm³	Flux, 10^{14} nv (≥1 Mev)	Dosage, 10^{21} nvt (≥1 Mev)	Length	Diameter	Volume		10^6 psi	10^{12} dynes/cm²	Percent of Unirradiated	10^6 psi	10^{12} dynes/cm³	Percent of Unirradiated	
UOX+0.5 wt% MgO	4	2.60	2.7	1.2	0.4	0.5	1.4	0.7	39.8	2.74	97	16.0	1.10	97	0.24
			2.7	1.2	0.4	0.6	1.6	-	37.1	2.56	91	15.0	1.03	91	0.24
	5	2.75	2.5	1.1	0.3	0.5	1.3	0.3	46.0	3.17	92	18.6	1.28	97	0.24
		2.90	2.4	1.1	0.6	0.3	1.2	~0	51.6	3.56	99	21.0	1.45	98	0.23
			2.8	1.3	0.4	0.3	1.1	~0	52.4	3.61	98	21.5	1.48	98	0.22
			2.9	1.3	0.4	0.4	1.1	0.1	50.7	3.50	96	21.0	1.45	97	0.21
	7		2.4	1.1	0.4	0.3	1.0	~0	52.8	3.64	98	21.3	1.47	99	0.24
			2.6	1.2	0.7	0.4	1.4	~0	53.3	3.67	98	21.5	1.48	99	0.24
AOX	8		2.7	1.2	0.3	0.5	1.2	0.5	48.1	3.32	93	19.8	1.36	94	0.22
UOX+3 wt% ZrO_2	5		2.5	1.1	0.4	0.5	1.5	~0	48.5	3.34	92	19.9	1.37	92	0.22
			2.3	1.0	0.5	0.5	1.6	0.4	48.0	3.39	93	19.9	1.37	92	0.23
			2.9	1.3	0.6	0.4	1.3	~0	50.2	3.46	95	20.6	1.42	92	0.22
UOX+1 wt% low silica glass	4		2.2	1.0	0.5	0.6	1.6	~0	49.3	3.40	97	20.4	1.41	97	0.21
			1.9	0.9	0.4	0.5	1.5	0.1	49.2	3.39	97	20.4	1.41	97	0.20
	5		2.8	1.3	0.7	0.6	2.0	~0	48.5	3.34	96	20.2	1.39	95	0.20
	17		2.3	1.0	0.4	0.4	1.2	0.1	49.8	3.43	96	20.4	1.41	96	0.22
UOX+1 wt% medium silica glass	9		2.0	0.9	0.5	0.6	1.7	0.2	48.3	3.33	92	19.8	1.36	92	0.22
			2.4	1.1	0.7	0.8	2.4	~0	-	-	-	-	-	-	-
	20		2.1	1.0	0.4	0.4	1.2	-	49.6	3.42	91	20.0	1.38	91	0.24
			2.2	1.0	0.7	0.6	1.9	-	47.8	3.30	88	19.3	1.33	88	0.24
UOX+1 wt% high silica glass	17		1.8	0.8	0.5	0.5	1.6	~0	51.7	3.56	97	21.1	1.45	96	0.23
			2.6	1.2	0.5	0.6	1.7	~0	51.2	3.53	96	20.9	1.44	95	0.22
UOX+2 wt% Bentonite glass	7		2.4	1.1	0.8	0.6	2.1	-	40.6	2.80	89	16.7	1.15	91	0.21
			2.1	1.0	0.8	0.5	1.9	-	42.3	2.92	93	17.5	1.21	93	0.21
			2.9	1.3	1.0	0.8	2.5	-	40.9	2.82	88	16.6	1.14	90	0.21
UOX+1 wt% Al_2O_3	5		2.2	1.0	-	1.0	-	-	36.2	2.50	77	15.3	1.05	84	0.18
			2.7	1.2	1.2	1.0	3.3	8 - 10	31.8	2.19	68	14.2	0.98	77	0.12
			2.6	1.2	1.3	1.0	3.4	8 - 10	37.6	2.59	80	15.7	1.08	85	0.20
EBOR (B78-33)	29	2.8	2.4	1.1	0.3	0.4	1.0	~0	45.8	3.16	97	19.1	1.32	97	0.20
(B86-47)	29	2.8	2.5	1.1	0.5	0.7	1.9	1.0	44.2	3.05	92	18.4	1.27	93	0.20
(B87-107)	26	2.8	2.6	1.2	0.4	0.5	1.3	-	46.7	3.22	99	19.4	1.34	96	0.20
			2.7	1.2	0.4	0.4	1.2	-	45.3	3.12	97	20.4	1.41	104	0.20

AOX, and UOX-ZrO_2 compositions. Changes in the glass-containing compositions ranged from slightly larger than the non-glass materials to some of the largest values that occurred. Changes in the glass phase materials did not appear strongly dependent on the grain size. Expansion of the EBOR material (22- to 28-micron grain size) was comparable to that of the non-glass compositions; in contrast, in the UOX-medium silica glass composition, expansion of the 20-micron grain size material was less than that in the 7-micron grain size. The largest expansion occurred in this latter material, in the UOX-2 weight percent bentonite, and in the UOX-Al_2O_3.

Open porosity changes, based in this instance on comparison with specimens from the same sintering batch rather than with pre-irradiation measurements on the same specimens, appeared significant in only one or two instances. The large increase in open porosity in the UOX-Al_2O_3 material indicates extensive microcracking.

The elastic constants decreased 10 to 15 percent compared to the pre-irradiation values. Changes of this magnitude are not conclusive evidence for microcracking but do indicate that microcracking is not extensive.

Microstructure Examinations

Polished sections of EBOR and AOX specimens of 20-micron grain size irradiated at 1000°C to 2.5 to 3 x 10^{21} nvt ($\geq$ 1 Mev) were examined by light and electron microscopy. As noted in the previous report,[4] strength decreases of 20 to 40 percent in these materials were considered indicative of microcracking since, in previous observations, the two phenomena were always associated.

Although some areas of the light micrographs were questionable, no evidence of microcracking was found in the electron micrographs. In representative areas of the samples, shown in Figure 5.2, the grain boundaries are tight and are visible only because of relief polishing. Further examinations are being made since these samples possibly represent the first instance of appreciable strength changes without microcracking.

WORK PLANNED FOR NEXT PERIOD

Examinations of the specimens irradiated in test 33MT111 (1000°C, ~4 x 10^{21} nvt) will be completed. Examinations will be made of the various BeO and BeO + Be compositions irradiated at 100°C to dosages up to about 5 x 10^{20} nvt.

[4] "High-Temperature Materials Program Progress Report No. 46, Part A," GE-NMPO, GEMP-46A, April 15, 1965, pp. 21–27.

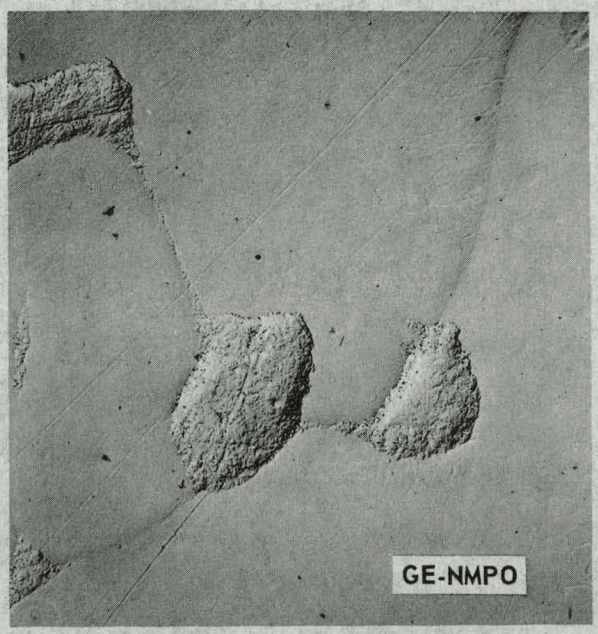

a – Unirradiated *(Neg. 850D, 5000X)*

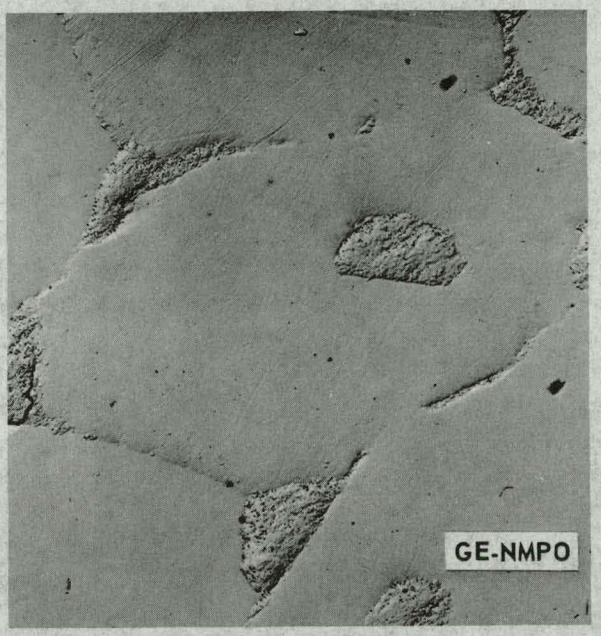

b – Irradiated *(Neg. 852E, 5000X)*

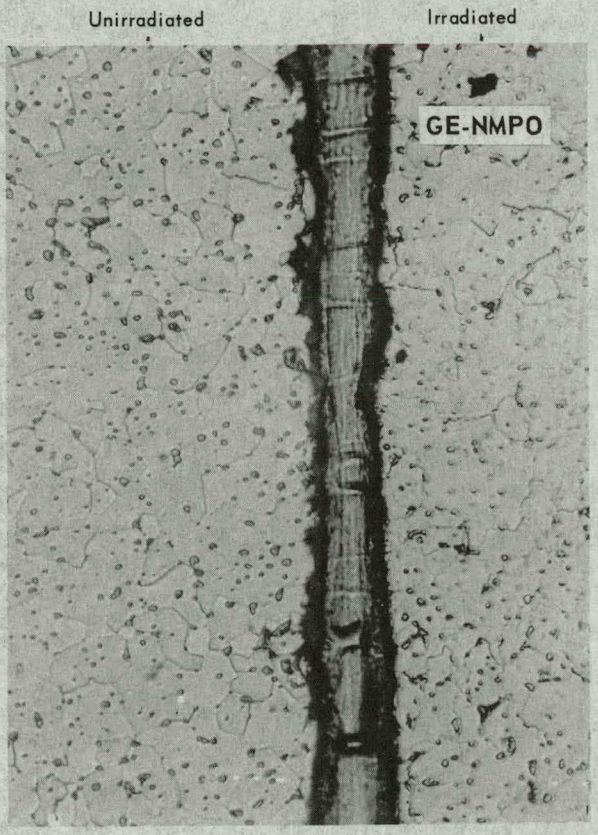

c – Light micrograph *(Neg. R1181, 250X)*

Fig. 5.2 – Electron and light micrographs of EBOR composition BeO irradiated at 1000°C to 2.9×10^{21} nvt ($\geq$1 Mev). No clear evidence of microcracking is apparent despite u decrease in strength of 20 to 40 percent

6. APPENDIX

The "High-Temperature Materials Program Progress Reports" previously issued in this series are listed below. The first two reports were each issued as one document, containing both the classified and unclassified portions. The subsequent reports were issued as two documents; part A, the unclassified portion and part B, the classified portion.

Report No.	Report Period	Publication Date
GEMP-1	May 1961 - June 30, 1961	July 15, 1961
GEMP-2	July 1, 1961 - July 31, 1961	August 15, 1961
GEMP-3, A and B	July 1, 1961 - August 31, 1961	September 15, 1961
GEMP-4, A and B	August 1, 1961 - September 30, 1961	October 15, 1961
GEMP-5, A and B	August 15, 1961 - October 15, 1961	November 15, 1961
GEMP-6, A and B	September 15, 1961 - November 15, 1961	December 15, 1961
GEMP-7, A and B	October 15, 1961 - December 15, 1961	January 15, 1962
GEMP-106, A and B (First Annual Report)	Calendar Year 1961	February 28, 1962
GEMP-9, A and B	January 1, 1962 - February 15, 1962	March 30, 1962
GEMP-10, A and B	January 1, 1962 - March 15, 1962	April 16, 1962
GEMP-11, A and B	February 15, 1962 - April 15, 1962	May 15, 1962
GEMP-12, A and B	March 15, 1962 - May 15, 1962	June 15, 1962
GEMP-13, A and B	April 15, 1962 - June 15, 1962	July 31, 1962
GEMP-14, A and B	May 15, 1962 - July 15, 1962	August 15, 1962
GEMP-15, A and B	June 15, 1962 - August 15, 1962	September 15, 1962
GEMP-16, A and B	July 15, 1962 - September 15, 1962	October 15, 1962
GEMP-17, A and B	August 15, 1962 - October 15, 1962	November 15, 1962
GEMP-18, A and B	September 15, 1962 - November 15, 1962	December 14, 1962
GEMP-19, A and B	October 15, 1962 - December 15, 1962	January 25, 1963
GEMP-177, A and B (Second Annual Report)	Calendar Year 1962	February 28, 1963
GEMP-21, A and B	January 1, 1963 - February 15, 1963	April 23, 1963
GEMP-22, A and B	January 1, 1963 - March 15, 1963	April 30, 1963
GEMP-23, A and B	February 15, 1963 - April 15, 1963	May 31, 1963
GEMP-24, A and B	March 15, 1963 - May 15, 1963	June 28, 1963
GEMP-25, A and B	April 15, 1963 - June 15, 1963	July 31, 1963
GEMP-26, A and B	May 15, 1963 - July 15, 1963	August 16, 1963
GEMP-27, A and B	June 15, 1963 - August 15, 1963	September 30, 1963
GEMP-28, A and B	July 15, 1963 - September 15, 1963	November 11, 1963
GEMP-29, A and B	August 15, 1963 - October 15, 1963	November 29, 1963
GEMP-30, A and B	September 15, 1963 - November 15, 1963	December 31, 1963
GEMP-31, A and B	October 15, 1963 - December 15, 1963	January 24, 1964
GEMP-270, A and B (Third Annual Report)	January 1, 1963 - January 31, 1964	February 28, 1964

Report No.	Report Period	Publication Date
GEMP-34, A and B	February 1, 1964 - March 15, 1964	April 15, 1964
GEMP-35, A and B	February 1, 1964 - April 15, 1964	May 28, 1964
GEMP-36, A and B	March 15, 1964 - May 15, 1964	June 19, 1964
GEMP-37, A and B	April 15, 1964 - June 15, 1964	July 31, 1964
GEMP-38, A and B	May 15, 1964 - July 15, 1964	August 19, 1964
GEMP-39, A and B	June 15, 1964 - August 15, 1964	September 30, 1964
GEMP-40, A and B	July 15, 1964 - September 15, 1964	October 15, 1964
GEMP-41, A and B	August 15, 1964 - October 15, 1964	November 30, 1964
GEMP-42, A and B	September 15, 1964 - November 15, 1964	December 18, 1964
GEMP-43, A and B	October 15, 1964 - December 15, 1964	January 29, 1965
GEMP-334, A and B (Fourth Annual Report)	January 31, 1964 - January 31, 1965	February 26, 1965
GEMP-46, A and B	February 1, 1965 - March 15, 1965	April 15, 1965
GEMP-47, A and B	February 1, 1965 - April 15, 1965	May 28, 1965

ATOMIC PRODUCTS DIVISION

GENERAL ELECTRIC